AD-A151 166 EHF ATTENUATION DERIVED FROM EMISSION TEMPERATURES IN LIGHT RAIN. (U) AEROSPACE CORP EL SEGUNDO CA ELECTRONICS RESEARCH LAB F I SHIMABUKURO ET AL. 1/1

UNCLASSIFIED 31 DEC 84 TR-0084A(5925-05)-1 SD-TR-84-58 F/G 4/2 NL

END

FILMED

DTIC

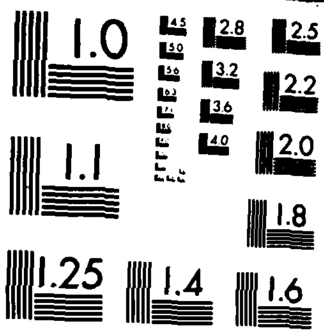

MICROCOPY RESOLUTION TEST CHART
NATIONAL BUREAU OF STANDARDS-1963-A

REPORT SD-TR-84-58

AD-A151 166

DTIC FILE COPY

EHF Attenuation Derived from Emission Temperatures in Light Rain

F. I. SHIMABUKURO and M. T. TAVIS
Electronics Research Laboratory

and

D. S. CHANG
Space Sciences Laboratory

Laboratory Operations
The Aerospace Corporation
El Segundo, CA 90245

31 December 1984

APPROVED FOR PUBLIC RELEASE;
DISTRIBUTION UNLIMITED

Prepared for

SPACE DIVISION
AIR FORCE SYSTEMS COMMAND
Los Angeles Air Force Station
P.O. Box 92960, Worldway Postal Center
Los Angeles, CA 90009-2960

85 03 05 006

This report was submitted by The Aerospace Corporation, El Segundo, CA 90245, under Contract No. F04701-83-C-0084 with the Space Division, P.O. Box 92960, Worldway Postal Center, Los Angeles, CA 90009. It was reviewed and approved for The Aerospace Corporation by D. H. Phillips, Director, Electronics Research Laboratory.

Lt. J. Morgan (CGX) was the project officer for the Mission-Oriented Investigation and Experimentation (MOIE) Program.

This report has been reviewed by the Public Affairs Office (PAS) and is releasable to the National Technical Information Service (NTIS). At NTIS, it will be available to the general public, including foreign nationals.

This technical report has been reviewed and is approved for publication. Publication of this report does not constitute Air Force approval of the report's findings or conclusions. It is published only for the exchange and stimulation of ideas.

LeROY C. YOUNG, Colonel, USAF
Director, Systems Engineering and
Advanced Space Communications
Deputy Commander for Space Systems

Joseph Hess, GM-15, Director, West Coast
Office, AF Space Technology Center

UNCLASSIFIED

SECURITY CLASSIFICATION OF THIS PAGE (When Data Entered)

REPORT DOCUMENTATION PAGE

READ INSTRUCTIONS BEFORE COMPLETING FORM

1. REPORT NUMBER SD-TR-84-58	2. GOVT ACCESSION NO.	3. RECIPIENT'S CATALOG NUMBER
4. TITLE (and Subtitle) EHF ATTENUATION DERIVED FROM EMISSION TEMPERATURES IN LIGHT RAIN		5. TYPE OF REPORT & PERIOD COVERED 6. PERFORMING ORG. REPORT NUMBER TR-0084A(5925-05)-1
7. AUTHOR(s) Fred I. Shimabukuro, Michael T. Tavis, and Dorothy S. Chang		8. CONTRACT OR GRANT NUMBER(s) F04701-83-C-0084
9. PERFORMING ORGANIZATION NAME AND ADDRESS The Aerospace Corporation El Segundo, Calif. 90245		10. PROGRAM ELEMENT, PROJECT, TASK AREA & WORK UNIT NUMBERS
11. CONTROLLING OFFICE NAME AND ADDRESS Space Division Los Angeles Air Force Station Los Angeles, Calif. 90009-2960		12. REPORT DATE 31 December 1984 13. NUMBER OF PAGES 28
14. MONITORING AGENCY NAME & ADDRESS(if different from Controlling Office)		15. SECURITY CLASS. (of this report) Unclassified 15a. DECLASSIFICATION/DOWNGRADING SCHEDULE

16. DISTRIBUTION STATEMENT (of this Report)

Approved for public release; distribution unlimited.

17. DISTRIBUTION STATEMENT (of the abstract entered in Block 20, if different from Report)

18. SUPPLEMENTARY NOTES

19. KEY WORDS (Continue on reverse side if necessary and identify by block number)

EHF attenuation from emission measurements in rain
Scattering in rain
Emission from rain at EHF
Rain attenuation at EHF

20. ABSTRACT (Continue on reverse side if necessary and identify by block number)

Atmospheric emission measurements have routinely been used to determine the total attenuation on an earth-space path at the centimeter and millimeter wavelengths. In the presence of rain, scattering effects have to be taken into account at frequencies > 20 GHz when one interprets emission data to derive the total attenuation. If one uses the radiometric relation to derive the attenuation, assuming an absorptive medium, one finds that the predicted attenuation underestimates the true attenuation. The reason for

DD FORM 1473 (FACSIMILE)

UNCLASSIFIED

SECURITY CLASSIFICATION OF THIS PAGE (When Data Entered)

19. KEY WORDS (Continued)

20. ABSTRACT (Continued)

this is that the rain scatters more emission energy out of the direct ray path than into it. Calculations of the atmospheric emission temperature and attenuation in light-to-moderate rain at different frequencies and rain rates are performed, taking into account molecular absorption, and varying cloud cover and ground temperature. The results show that for typically encountered meteorological conditions, the radiometric formula can be used to derive the total attenuation (< 10 dB) from emission measurements with accuracies of the order less than 1 dB, provided that the empirical constant in the radiometric formula, dependent on the ambient temperature, is a function of frequency and ground temperature.

ACKNOWLEDGMENT

The authors thank N. E. Feldman for his support and encouragement in this study.

A-1

CONTENTS

FIGURES

TABLES

I. INTRODUCTION

Atmospheric emission measurements have been used to determine the total attenuation in rain on an earth-to-space path at the centimeter and millimeter wavelengths (Wilson, 1969; Wulfsberg and Altshuler, 1972; Meyerhoff et al., 1974; Hogg and Chu, 1975; Meyerhoff, 1975; Brussaard, 1977; Lin et al., 1979; Ishakov et al., 1980; Babkin et al., 1982). If the propagating medium is entirely absorptive, the attenuation can be obtained by inverting the equation of radiative transfer, which, for radio wavelengths, can be expressed as

$$T_e = \int_0^{\tau_0} T_e^{-\tau} d\tau \qquad (1)$$

where T_e is the measured emission temperature, T is the temperature of the medium, τ is the opacity ($d\tau = \alpha dx$), α is the absorption coefficient, and x is the distance along the ray path. If T is a constant, T_0 [Eq. (1)] reduces to the usual radiometric formula

$$T_e = T_0(1 - e^{-\tau_0}) \qquad (2)$$

and the total opacity is given by

$$\tau_0 = \ln\left(\frac{T_0}{T_0 - T_e}\right) \qquad (3)$$

and A, the attenuation in decibels, is given by 4.34 τ_0. In the atmosphere, the temperature changes with height, but not by a large percentage (typically less than 10%) in the region where most of the attenuation takes place. Thus, in practice, an effective medium temperature T_m is used, and Eq. (3) gives a good measure of the atmospheric attenuation, with errors typically less than 1 dB, in the range of attenuations less than 12 dB. T_m is substituted for the term T_0 in the equation.

In the presence of rain, scattering effects have to be taken into account at frequencies > 20 GHz when one interprets emission data to derive the total attenuation. The relative significance of the scattering effects can be seen in Fig. 1, which shows the absorption-to-extinction ratio as a function of frequency in light-to-moderate rain, assuming a Marshall-Palmer [1948] drop-size distribution. Zavody [1974] showed that, at millimeter wavelengths, attenuations derived from emission observations can be significantly low if the attenuation in rain is assumed to be due only to absorption. Calculations of atmospheric emission in rain were made at 37, 72, and 110 GHz at three elevation angles, taking into account multiple scattering, including ground contributions. An isothermal atmosphere (273 K) was assumed, with a 3-km-thick rain layer. The ground temperature was the same as the atmosphere. In the calculation, molecular - but not cloud - effects were included.

Chadha and Lane [1977] used a sun-tracking 37-GHz radiometer to measure the attenuation during rain, first directly, using the sun as a source, and second, using emission measurements. They found that the attenuations derived from the emission measurements, assuming a purely absorptive medium, under-estimated the true attenuation by 10 to 15% for vertical polarization and by 30 to 35% for horizontal polarization at elevation angles in the range of 10 to 35 degrees. These results are in reasonable agreement with the predictions of Zavody [1974] for horizontal polarization, but the theory overestimates the attenuation for vertical polarization.

Ishimaru and Cheung [1980] calculated atmospheric emission in rain from the equation of radiative transfer using a scattering matrix approach. They calculated the emissions for vertical and horizontal polarizations at 30, 60, 90, and 120 GHz (at various elevation angles and for rainfall rates of 0.25 and 12.5 mm/hr) for 1-km and 3-km rain layers, assuming a constant rain temperature of 273 K. The ground temperature was 283 K, with an albedo of 0.5. Molecular and cloud effects were not included in the formulation. The results are in good agreement with the measurements of Chadha and Lane [1977]. In the papers by Zavody [1974] and Ishimaru and Cheung [1980], a Laws-Parsons [1943] drop-size distribution was assumed for rain.

In this report we calculate the atmospheric emission and attenuation at various frequencies in light-to-moderate rain, and investigate the errors in

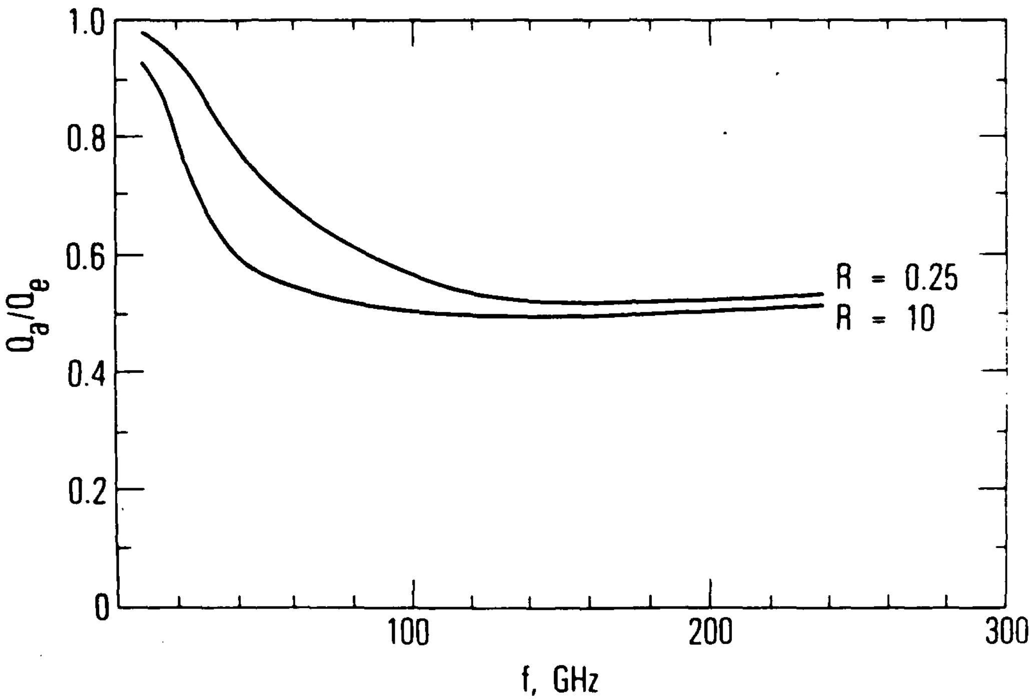

Fig. 1. Curves showing the ratio of the absorption (Q_a) to extinction (Q_e) coefficients for rain, assuming a Marshall-Palmer drop-size distribution. Curves are shown for two rain rates, R = 0.25 and R = 10 mm/hr.

the attenuation derived from emission measurements when the weather conditions and measurement geometry vary. A stratified atmosphere is assumed.

II. FORMULATION

The atmospheric model used in the calculations is shown in Fig. 2. The mission temperatures are computed at zero height from a zenith direction, . The ground has unit emissivity at a temperature T_g. The atmospheric temerature is T_g at h = 0 and decreases linearly at a rate that gives a temerature of 273 K at h_1 (h_1 = 3 km), which height is the top of the rain layer nd bottom of the clouds. The top of the cloud layer is at h_2 ($h_2 - h_1$ = 1 m), and the cloud liquid-water content is LWC. At the wavelengths conidered, the cloud medium is absorptive, and the expression for attenuation is ;iven by Gunn and East [1954], as

$$\alpha_c = 8.186 \frac{LWC}{\lambda} \mathrm{Im} \left(- \frac{m^2 - 1}{m^2 + 2}\right) \text{ dB/km} \tag{4}$$

where Im means the imaginary part, LWC is the liquid content in g/m^3, λ is the wavelength in cm, and m is the complex index of refraction for liquid water at 273 K. The pressure is 1013 mb at the surface and drops off exponentially with a scale height of 8.4 km. The water vapor density was assumed to be that for a 100 percent relative humidity at all heights. The oxygen absorption was simply characterized with two lines of equal linewidth, one centered at zero frequency and one centered at 60 GHz [Van Vleck, 1947] using the Van Vleck-Weisskopf [1945] lineshape and line parameter constants of Ho et al. [1972]. The absorption coefficient for water vapor was calculated from the formula of Waters [1976]. The oxygen line at 118 GHz and the water vapor line at 183 GHz were not included in the formulation, since these lines had negligible effect on the attenuations at the frequencies where the computations were made. The molecular effects are included from the surface to a height of 5 km. The rain layer was assumed to be of infinite horizontal extent and the index of refraction of the rain droplets was given by the formula of Ray [1972] for liquid water at a temperature $T = \frac{1}{2}(T_g + 273)$.

The procedure for calculating the emission temperature follows that given by Zavody [1974]. The main differences are that in this report, a linear y Oguchi [1960, 1964], and subsequently by others. The differential attenua- ion of horizontally and vertically polarized waves through rain is a function ıf frequency, rain rate, and elevation angle. From the results of Morrison ınd Chu [1973] and Chu [1974] for the meteorological conditions considered in :his study, the largest differential attenuation occurs for R = 10 mm/hr at 44 ;Hz, and amounts to ~ 0.4 dB/km. If accuracies in the determination of the ıttenuation of the order of 1 dB are satisfactory, it appears that from esti- ıates of the rain rate and rain height, the differential attenuation correc- :ions as calculated by Morrison and Chu [1983] and Chu [1974] can be applied to the unpolarized results and correct for the effect of non-spheroidal drops on polarized waves.

The results of this study can be applied to the 37-GHz attenuation measurements of Chadha and Lane [1977]. In Fig. 8 are shown the best-fit curves for the measured attenuations for horizontal and vertical attenuations. The bottom curve is the predicted attenuation, and uses the radiometric formula and a value of T_m estimated from local meteorological data (based on temperature and type of rainfall). The values of T_m used were in the range 273 to 280 K. From Eq. (7), the modified values of T_m at 37 GHz are 261 K and 265 K for ground temperatures of 273 K and 280 K, respectively. Using the modified values of T_m obtained from Eq. (7), the predicted attenuations for unpolarized signals are plotted as range bars, using the measured emission data of Chadha and Lane [1977]. It is seen that there is a reasonably good agreement between the measurements and the predicted attenuations from this study.

The column marked σ is the standard deviation of the T_m's in the attenuation range between 9 and 11 dB. At 10 and 16 GHz, the attenuations are less than 9 dB in all cases, and no entries for this parameter are given for these frequencies. The derivative $\frac{dA}{dT_m}$ gives the sensitivity of the derived attenuation to errors in T_m. For $T_m = 273$ K and A = 10 dB, $\left|\frac{dA}{dT_m}\right| = 0.14$ dB/K, indicating that for the conditions here, emission measurements can be used to determine atmospheric attenuations at EHF, i. the range less than 10 dB, with standard errors less than 1 dB.

If the meteorological conditions encountered in practice generate T_m's with greater variabilities than those modeled in this study, the errors in the derived attenuations will be correspondingly greater. If this occurs, in order to improve the accuracy in the determination of the attenuation using emission measurements, the value of T_m will have to be more accurately determined. Information about the rain rate, rain height, elevation angle, and cloud liquid-water content could be utilized. The elevation angle and surface rain rate are directly measurable, but the integrated rain rate, rain height, and cloud LWC can only be estimated indirectly. Estimates or perhaps bounds of the LWC, the rain height, and the integrated rain rate can be obtained from the surface rain rate and from statistical weather data of the particular geographic location, or from multifrequency emission measurements. Utilization of these data will decrease the errors in the attenuation by the determination of a better estimate of T_m in the radiometric relation.

There is one further correction that has to be applied, and that is for polarization. The calculations here have been performed for spherical rain drops and for unpolarized signals. The fact is that rain drops falling at their terminal velocity are not spherical but are approximately oblate spheroids, [Pruppacher and Pitter, 1971] and, in atmospheric conditions, the major axes of the droplets are canted at some small angle from the horizontal. The result is that on a propagation path in the atmosphere through rain, horizontally polarized signals are attenuated more strongly than vertically polarized signals. The effect of oblate raindrops on propagation was first studied

The values of the derived T_m do not have much scatter for $f < 20$ GHz, and one can conclude that radiometric measurements will be most accurate for determining attenuation at these frequencies. For $f > 30$ GHz, there is increased scatter, with a corresponding decrease in the accuracy. A measure of the accuracy of the emission method for the determination of attenuation is given by the standard deviation of T_m. The plots show a dependence on T_g for which a correction can be applied, and the statistics given will be derived for the cases where $T_g = 290$.

For the meteorological conditions considered in this study, emission measurements can be used to determine the atmospheric attenuation in rain at EHF within 1 dB for zenith angles less than 70 degrees, and for attenuation levels less than 10 dB. In order to accomplish this, the parameter T_m in Eq. (3) needs to be a function of frequency and ground temperature. A simple form is given by

$$T_m(f,T_g) = T_1(f) + 0.6(T_g - 290) \tag{7}$$

In Table 1, the values of $T_1(f)$ derived for the stated meteorological conditions are listed. The attenuations for 220 GHz were greater than 10 dB in all cases, and the parameters for this frequency were not included in the table.

Table 1. T_m in Radiometric Formula

$T_m = T_1(f) + 0.6(T_g - 290)$

Frequency, GHz	$T_1(f)$	σ ($9 < A < 11$ dB)
10	275	
16	274	
20	274	1.1
30	272	2.1
44	271	3.2
90	268	2.0
140	272	3.5

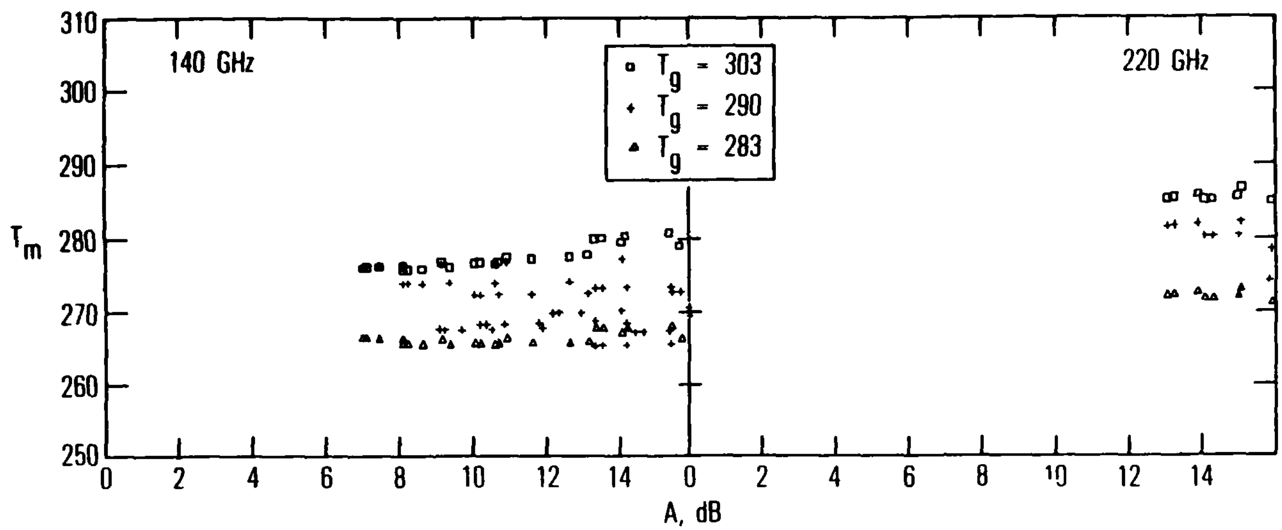

Fig. 7. Derived T_m's for the calculated emission temperatures and attenuations.

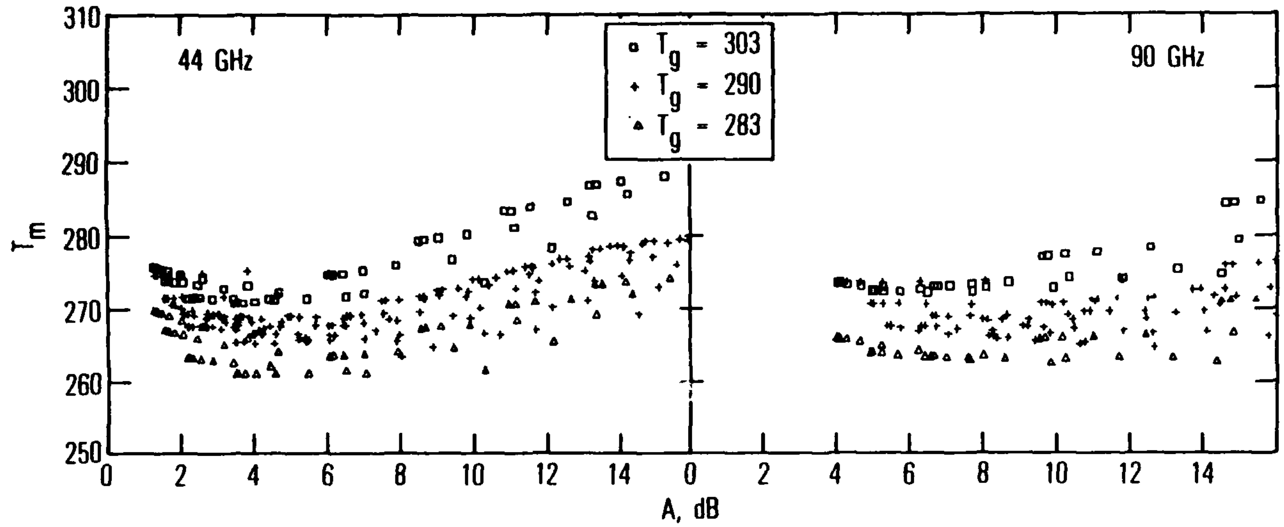

Fig. 6. Derived T_m's for the calculated emission temperatures and attenuations.

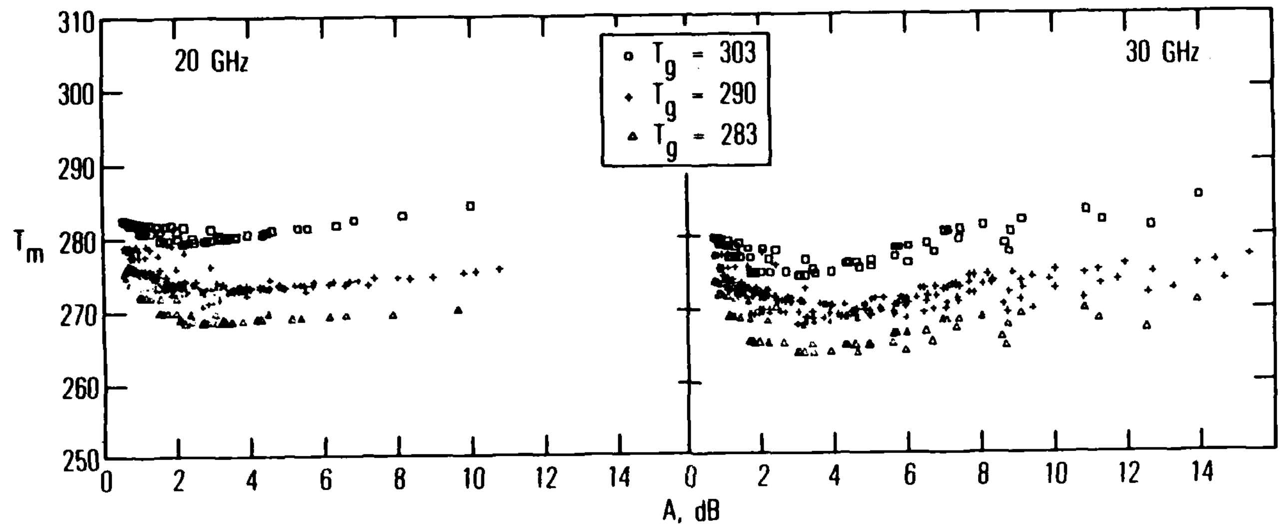

Fig. 5. Derived T_m's for the calculated emission temperatures and attenuations.

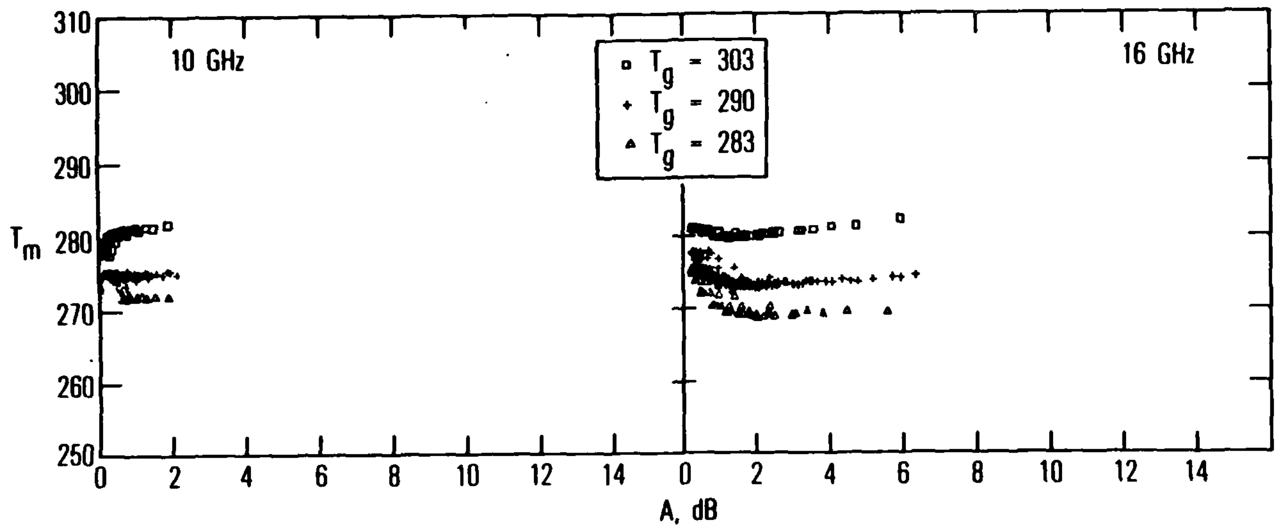

Fig. 4. Derived T_m's for the calculated emission temperatures and attenuations.

and 12 dB, respectively. Suppose, for a given application, attenuations up to, say, a maximum of 10 dB are to be determined by radiometric measurements. Then, the best fit T_m for the 10-dB level should be used in the radiometric formula. This minimizes the error at the maximum attenuations, noting that errors in the attenuation at the lower levels are not as sensitive to improper values of T_m.

In Figs. 4-7 are plotted the values of T_m (for $A < 15$ dB and $z < 70$ degrees) for the different frequencies. These T_m's are derived from the calculated attenuations and emission temperatures using the radiometric formula, for the five cases listed above. The scatter in T_m gives an indication of the accuracy with which atmospheric attenuations can be determined by emission measurements. In the plots the crosses are obtained from cases 1, 2, and 3, those cases with different cloud covers but with the same ground temperature $T_g = 290$ K. The triangles and boxes are obtained from cases 4 and 5, respectively.

A few observations can be made about emission temperatures in rain. The variation in emission temperature for the same attenuation increases as the scattering effects increase. In the frequency range between 20 and 140 GHz, the scattering-to-extinction ratio for rain changes significantly as the rain rate increases from 0.25 to 10 mm/hr (see Fig. 1). The relatively high values of T_m in this frequency range for low attenuations occur at $R = 0.25$. At this rain rate the attenuation due to absorption dominates and the emission temperature is highest for a given attenuation. As the rain rate increases, the scattering effects increase and T_m decreases. When the scattering effects are significant, say $Q_s/Q_e > 0.3$ where Q_s and Q_e are the rain scattering and extinction coefficients, respectively, clouds can noticeably affect the value of T_m which satisfies the radiometric relation. If the cloud absorption is a sizable fraction of the total attenuation, a significant fraction of the cloud emission gets scattered out of the direct ray path without fully compensating multiple scattering contributions, and lower values of T_m result. The lowest values of T_m in the plots occur for low rain rates, the largest LWC, and at the largest secant angles.

energy scattered out of the direct ray path is greater than the energy scattered into it. This is the reason the use of the radiometric formula in rain conditions will underestimate the true attenuation if one assumes the medium to be absorptive. This has been noted in previous studies (e.g., Wilson, 1969; Gray, 1972; Zavody, 1974; Hogg and Chu, 1975). If, for the given meteorological conditions, one is able to determine an effective radiometric medium temperature T_m, somewhat smaller than that derived for an absorptive medium, then emission measurements can be used to determine the atmospheric attenuation with sufficient accuracy, for certain applications.

The calculations show that if the radiometric relation given by Eq. (3) is to be used to determine the attenuation accurately in all conditions for a large range of attenuations, the parameter T_m, used in place of T_0 in Eq. (3), cannot be a constant, but is a function of frequency, rain rate, rain height, elevation angle, cloud cover, and ambient temperature. In practice, it would be desirable to have T_m dependent on as few parameters as possible, and in addition, these parameters should be measurable, or known quantities. Of the above quantities, the frequency, the elevation angle, and the ground temperature can be measured, whereas the integrated rain rate along the ray path, and the LWC in the clouds, are not directly measurable. So at most, T_m should be a function of frequency, zenith angle, and ground temperature. The errors in the attenuation derived from Eq. (3) arise from errors in the measurement of T_e and from using the wrong value of T_m in the radiometric formula.

With the present technology, well-designed radiometers at EHF have sensitivities and uncertainties in the absolute calibrations, which are less than 1 K for a one-second integration time. Therefore, the significant errors in the attenuations derived from emission measurements will not arise from the measurements themselves, but rather from the variability in the measurement geometry and in the meteorological conditions, which factors determine the proper value of T_m in the radiometric formula. For a given error in T_m, the error in the derived attenuation depends on the attenuation level. For example, for $T_m = 273$ K, in using Eq. (3), a 5-K error in T_m gives errors of 0.05 dB, 0.65 dB, and 1.0 dB in the attenuation at levels of 2 dB, 10 dB,

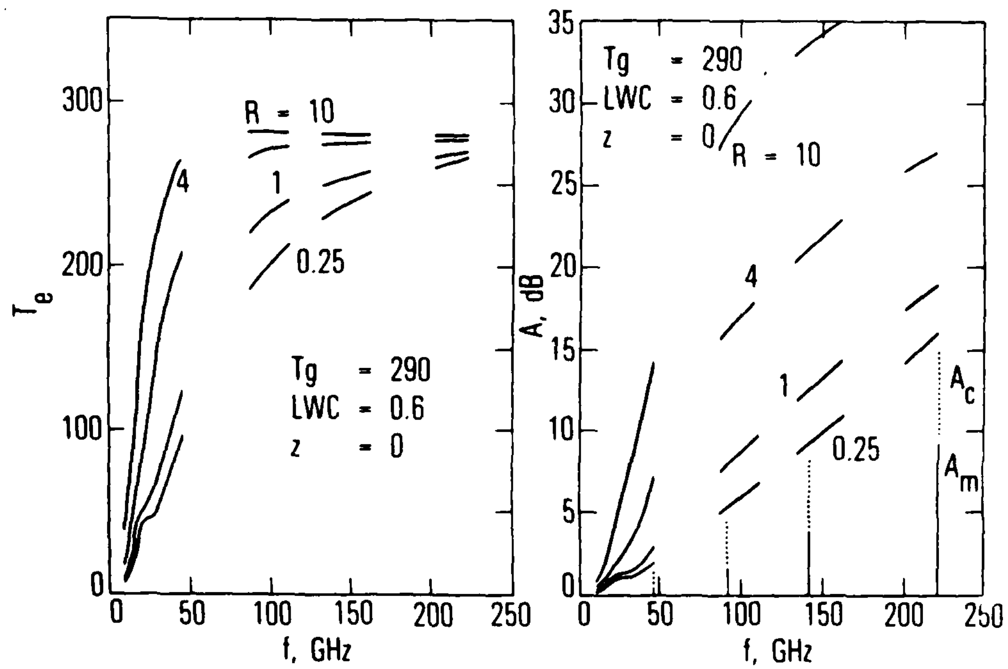

Fig. 3. Calculated emission temperatures and zenith attenuations.

III. RESULTS

The emission temperatures and attenuations of the atmosphere were calculated at zenith angles from 0 to 90 degrees, in 10 degree increments, at 10, 16, 20, 30, 44, 90, 140, and 220 GHz, for rain rates 0.25, 0.5, 1, 2, 4, 6, 8, and 10 mm/hr, for the following cases: (1) $T_g = 290$, LWC = 0.3; (2) $T_g = 290$, LWC = 0.6; (3) $T_g = 290$, LWC = 1.2; (4) $T_g = 283$, LWC = 0.3; and (5) $T_g = 303$, LWC = 0.3. We are primarily interested in the EHF region, but calculations at 10, 16, and 20 GHz are included for comparisons.

A plot of the calculated emission temperatures and attenuations in the zenith direction, as a function of frequency, for four of the rain rates for case 2 is shown in Fig. 3. Although the calculations were made at the eight discrete frequencies, smooth curved segments were drawn in the vicinity of these frequencies to indicate the trend and to help distinguish the curves of the different rain rates. Also shown in the attenuation plots are the fractional contributions of the molecular and cloud absorptions to the total attenuation for 44, 90, 140, and 220 GHz. The oxygen absorptions at these frequencies are relatively small, and are depicted by pedestals on the vertical lines marked A_m, the total molecular absorption. At the lower rain rates the cloud and molecular absorption are the main causes of attenuation and must be taken into account in the design of EHF satellite communication systems with small link margins.

In rain, a fraction of the energy emitted by the absorbing particles directly at the radiometer gets scattered out of the path and does not contribute to the measured emission temperature. However, the rain also scatters energy, including that from the ground, into the direct ray path, and the application of the radiometric formula for accurate attenuation measurements depends on the relative quantities of the two scattered energies described above, for different conditions. In typical meteorological conditions with rain, the emission temperature will be less than that obtained from a completely absorbing medium with the same total attenuation. In other words, the subdivision and self checking. Two-dimensional cubic splines are then used to approximate the function at arbitrary angles. Further simplifications are obtained by taking advantage of the assumed infinite horizontal extent of the rain, and cylindrical symmetry can be utilized. Also, the computations can be reduced by one fourth, by noting the following symmetries:

$$S(\theta,\zeta) = S(\zeta,\theta)$$

$$S(\theta,\zeta) = S(\pi-\zeta,\ \pi-\theta) \tag{6}$$

temperature gradient from the ground to the freezing level is assumed, and cloud effects are included. The formulation of Deirmendjian [1963] was used to calculate the scattering coefficients. The calculations are done for unpolarized radiation. Briefly, the emission temperature at each zenith angle z is given by

$$T_e(z) = \sum_{n=0}^{\infty} T_A^{(n)}(z) + \sum_{n=1}^{\infty} T_G^{(n)}(z) \tag{5}$$

where the first summation includes the temperature contributions from absorbers in the atmosphere, and the second summation gives the ground contributions scattered into the antenna beam. $T_A^{(0)}(z)$ is the temperature contribution of all absorbers in the direct ray path, extincted by absorption and scattering. The terms, $T_A^{(n)}(z)$, for $n \geq 1$, are the temperature contributions from energy scattered n times before it enters the antenna from the zenith direction z. Included are the emissions from the cloud layer and molecules above the rain, which get scattered within the rain layer. $T_G^{(n)}(z)$ are contributions resulting from ground emission multiply scattered by the rain. In the summations, all temperature contributions greater than 0.1 K are included.

At the higher frequencies and rain rates, up to eleven orders of scattering have to be taken into account. The computations were done in the following way. Given the physical properties of the rain, the scattering coefficient at a point is a function of a single variable, the scattering angle γ. This angle γ, in turn, can be expressed as a function of three angles at the scatterer: θ, the angle between the zenith and the incident ray; ζ, the angle between the zenith and the scattered ray; and ϕ, the azimuthal angle between the incident and scattered ray. The scattering coefficient is then made independent of ϕ by integrating over 2π, and is designated by $S(\theta,\zeta)$.

In the multiple-scattering computations, the function $S(\theta,\zeta)$ is used over and over again, and the computational time was reduced by the following procedure. $S(\theta,\zeta)$ is a smooth function and is evaluated every 10 deg in both the θ and ζ directions by using two-point Gaussian quadrature with interval

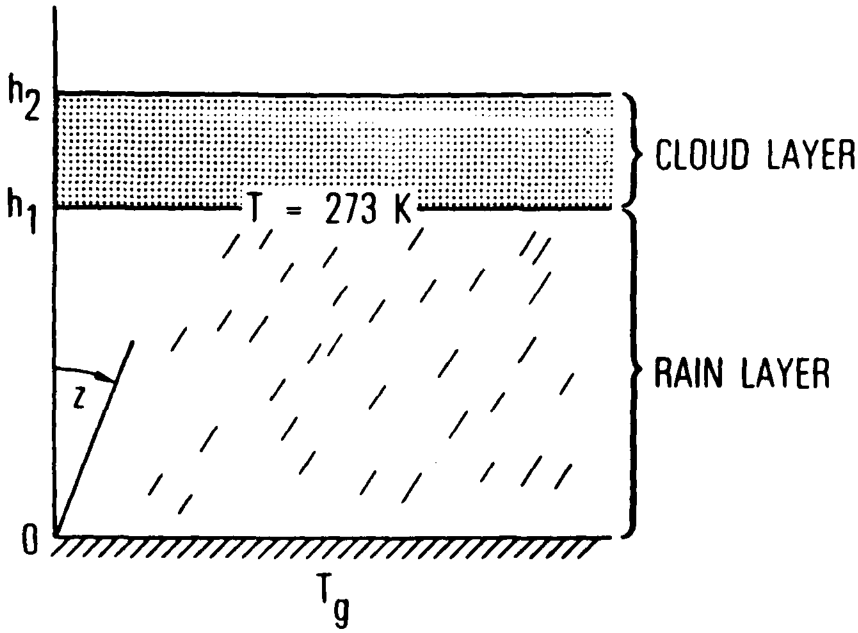

Fig. 2. Schematic of the rain model used for the emission and attenuation calculations.

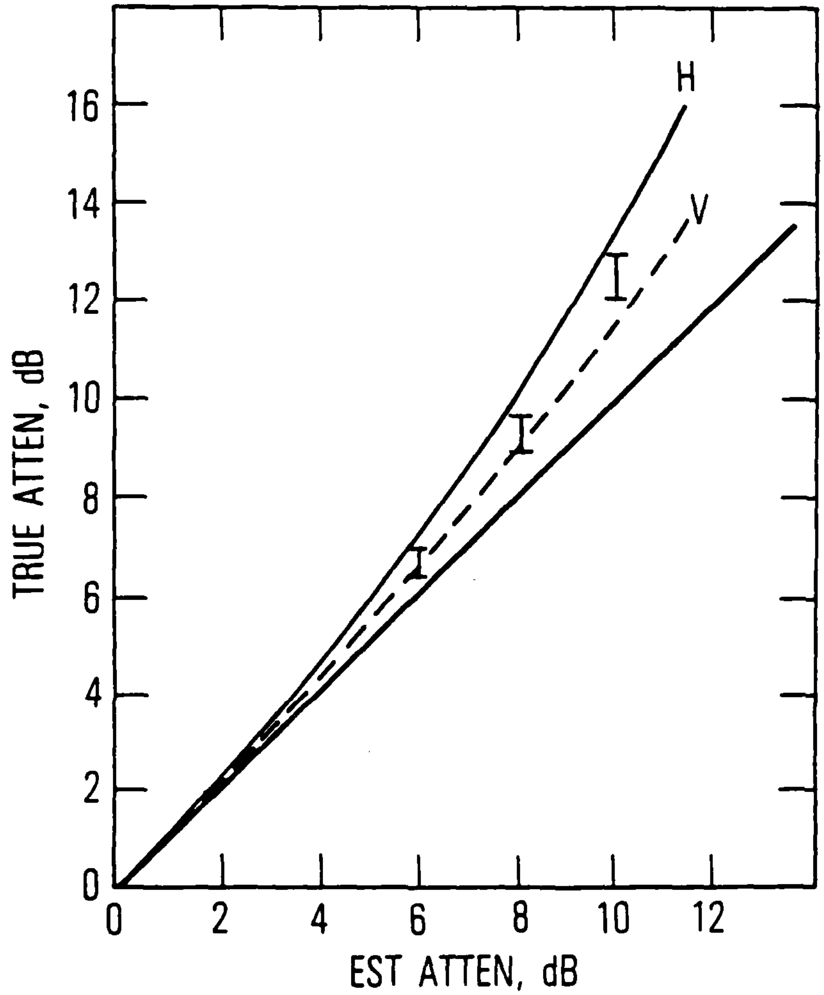

Fig. 8. Comparison of the predicted attenuations from the results of this study and the measurements of Chadha and Lane [1974].

IV. CONCLUSIONS

If emission measurements are used to determine atmospheric attenuation at EHF in rain, scattering effects must be taken into account when applying the radiometric formula to derive the attenuations. In order to obtain the attenuation from the radiometric formula in all conditions for a large range of attenuations, the effective medium temperature T_m cannot be a constant but is a function of frequency, rain rate, rain height, elevation angle, cloud cover, and ambient temperature. However, for applications requiring the determination of attenuations less than 10 dB with accuracies of the order of 1 dB, the use of a T_m in the radiometric formula which is a simple function of frequency and ground temperature will suffice, at least for the conditions considered in this study. The results are in agreement with reported measurements.

REFERENCES

1. Babkin, Yu. S., Ye. V. Sukhonin, and V. I. Chernyshev, "Results of the Annual Measurement Cycle of Vertical Atmospheric Attenuation at the Wavelength of 8.2 mm, Based on Internal Atmospheric Radiation," Radio Engineering and Electron. Phys. 27 (19-23 February 1982).

2. Brussaard, G., "Rain Attenuation on Satellite-Earth Paths at 11.4 and 14 GHz," Proc. URSI Symp., La Baule (1977), pp. 393-398.

3. Chadha, R., and J. A. Lane, "Effect of Scattering in Measurements of Rain Attenuation by Passive Radiometry," Electron. Lett. 13, 177-178 (1977).

4. Chu, T. S., "Rain-Induced Cross-Polarization at Centimeter and Millimeter Wavelength," BSTJ 53, 1557-1579 (1974).

5. Deirmendjian, D., "Complete Microwave Scattering and Extinction Properties of Polydispersed Cloud and Rain Elements," Rand Rept. R-422R (1963).

6. Gray, D. A., "The Relationship Between Satellite Signal Attenuation and Sky Temperature," USNC-URSI Abstracts, 22-23 (1972).

7. Gunn, K. L. S., and T. W. R. East, "The Microwave Properties of Precipitating Particles," Quant. J. Roy. Meteor. Soc. 80, 522-545 (1954).

8. Ho, W., H. H. Wang, W. F. Hall, W. Norris, W. N. Hardy, K. W. Gray, and G. M. Hidy, "Brightness Temperature of the Terrestrial Sky at 2.66 GHz," J. Atm. Sci. 29, 1210-1212 (1972).

9. Hogg, D. C., and T. S. Chu," The Role of Rain in Satellite Communications," Proc. IEEE 9, 1308-1330 (1975).

10. Ishakov, T. A., Ye. V. Sukhonin, and V. I. Chernyshev," Measurement of the Vertical Attenuation of 4.1-mm Radiation in the Earth's Atmosphere," Radio. Engineering and Electron. Phys. 25, (9-11 October 1980).

11. Ishimaru, A., and R. L. T. Cheung, "Multiple-Scattering Effect on Radiometric Determination of Rain Attenuation at Millimeter Wavelengths," Radio Science 15, 507-516 (1980).

12. Laws, J. O., and D. A. Parsons, "The Relation of Raindrop Size to Intensity," Trans. Amer. Geophys. U. 4, 452-460 (1943).

13. Lin, S. H., H. J. Bergmann, and M. V. Pursley, " Rain Attenuation on Earth-Satellite Paths - Summary of 10-Year Experiments and Studies," BSTJ 59, 183-228 (1979).

14. Marshall, J. S., and W. M. Palmer, "The Distribution of Raindrops with Size," Journ. of Met. 5, 165-166 (1948).

15. Meyerhoff, H. J., "11.7 and 20-GHz Radiometric Measurements at a Brazilian Equatorial Site," COMSAT Tech. Rev. 5, 399-411 (Fall, 1975).

16. Meyerhoff, H. J., A. Buige, and E. A. Robertson, "15.3-GHz Precipitation Attenuation Measurements Using a Transportable Earth Station at Uribe, Panama," COMSAT Tech. Rev. 4, 170-186 (Spring, 1974).

17. Morrison, J. A. and T. S. Chu, "Perturbation Calculations of Rain-Induced Differential Attenuation and Differential Phase Shift at Microwave Frequencies," BSTJ 52, 1907-1913 (1973).

18. Oguchi, T., "Attenuation of Electromagnetic Waves Due to Rain with Distorted Raindrops," J. Radio Res. 7, Part I, 467-485 (1960); J. Radio Res. 11, Part II, 18-44 (1964).

19. Pruppacher, H. R., and R. L. Pitter, "A Semi-Empirical Determination of the Shape of Cloud and Rain Drops," J. Atmos. Sci. 28, 86-94 (1971).

20. Ray, P. S., "Broadband Complex Refractive Indices of Ice and Water," App. Opt. 11, 1836-1844 (1972).

21. Van Vleck, J. H., "The Absorption of Microwaves by Oxygen," Phys. Rev. 71, 425-433 (1947).

22. Van Vleck, J. H., and V. F. Weisskopf, "On the Shape of Collision-Broadened Lines," Rev. Mod. Phys. 17, 227-236 (1945).

23. Waters, J. W., in M. L. Meeks, ed., Methods of Experimental Physics, Vol. 12B, Chap. 2.3 (Academic Press, New York, 1976).

24. Wilson, R. W. "Sun Tracker Measurements of Attenuation by Rain at 16 and 30 GHz," BSTJ 48, 1383-1404 (1969).

25. Wulfsberg, K. N., and E. E. Altshuler, "Rain Attenuation at 15 and 35 GHz," IEEE Trans. Antennas and Prop. AP-20, 181-187 (1972).

26. Zavody, A. M., "Effect of Scattering by Rain on Radiometer Measurements at Millimeter Wavelengths," Proc. IEEE 121, 257-263 (1974).

LABORATORY OPERATIONS

The Laboratory Operations of The Aerospace Corporation is conducting experimental and theoretical investigations necessary for the evaluation and application of scientific advances to new military space systems. Versatility and flexibility have been developed to a high degree by the laboratory personnel in dealing with the many problems encountered in the nation's rapidly developing space systems. Expertise in the latest scientific developments is vital to the accomplishment of tasks related to these problems. The laboratories that contribute to this research are:

Aerophysics Laboratory: Launch vehicle and reentry fluid mechanics, heat transfer and flight dynamics; chemical and electric propulsion, propellant chemistry, environmental hazards, trace detection; spacecraft structural mechanics, contamination, thermal and structural control; high temperature thermomechanics, gas kinetics and radiation; cw and pulsed laser development including chemical kinetics, spectroscopy, optical resonators, beam control, atmospheric propagation, laser effects and countermeasures.

Chemistry and Physics Laboratory: Atmospheric chemical reactions, atmospheric optics, light scattering, state-specific chemical reactions and radiation transport in rocket plumes, applied laser spectroscopy, laser chemistry, laser optoelectronics, solar cell physics, battery electrochemistry, space vacuum and radiation effects on materials, lubrication and surface phenomena, thermionic emission, photosensitive materials and detectors, atomic frequency standards, and environmental chemistry.

Electronics Research Laboratory: Microelectronics, GaAs low noise and power devices, semiconductor lasers, electromagnetic and optical propagation phenomena, quantum electronics, laser communications, lidar, and electro-optics; communication sciences, applied electronics, semiconductor crystal and device physics, radiometric imaging; millimeter wave, microwave technology, and RF systems research.

Information Sciences Research Office: Program verification, program translation, performance-sensitive system design, distributed architectures for spaceborne computers, fault-tolerant computer systems, artificial intelligence and microelectronics applications.

Materials Sciences Laboratory: Development of new materials: metal matrix composites, polymers, and new forms of carbon; nondestructive evaluation, component failure analysis and reliability; fracture mechanics and stress corrosion; analysis and evaluation of materials at cryogenic and elevated temperatures as well as in space and enemy-induced environments.

Space Sciences Laboratory: Magnetospheric, auroral and cosmic ray physics, wave-particle interactions, magnetospheric plasma waves; atmospheric and ionospheric physics, density and composition of the upper atmosphere, remote sensing using atmospheric radiation; solar physics, infrared astronomy, infrared signature analysis; effects of solar activity, magnetic storms and nuclear explosions on the earth's atmosphere, ionosphere and magnetosphere; effects of electromagnetic and particulate radiations on space systems; space instrumentation.

END

FILMED

5-85

DTIC